

1 **Marine phytoplankton in subtropical coastal**
2 **waters showing lower thermal sensitivity than**
3 **microzooplankton**

4

5 Kailin Liu¹, Bingzhang Chen², Shuwen Zhang³, Mitsuhide Sato¹,
6 Zhiyuan Shi¹, Hongbin Liu¹ *

7

8 ¹Department of Ocean Science, Hong Kong University of Science and Technology, Hong
9 Kong

10 ²Department of Mathematics and Statistics, University of Strathclyde, Glasgow, UK

11 ³College of Life Science, South China Normal University, 55 of Zhongshan West
12 Avenue, Guangzhou 510631, PR China

13 *Corresponding author: liuhb@ust.hk. Tel: +852-23587341, Fax: +852-23581559.

14 Key words: activation energy; optimal temperature; phytoplankton growth;
15 microzooplankton grazing

16 Running head: lower thermal sensitivity of phytoplankton

17

18 **Abstract**

19 Temperature sensitivity of plankton in terms of activation energy (E_a , eV) in the
20 Arrhenius equation is critical for predicting how marine productivity and carbon export
21 will respond to ocean warming. In this study, we quantified the temperature responses of
22 phytoplankton growth rate and microzooplankton grazing rate by conducting short-term
23 temperature modulation experiments on natural communities at two subtropical sites with
24 contrasting nutrient conditions. Our results showed that the activation energy of
25 phytoplankton growth rate ($E_a = 0.36$ eV, 95% CI = 0.28 to 0.44 eV) at each station was
26 less than that of microzooplankton grazing rate ($E_a = 0.53$ eV, 95% CI = 0.47 to 0.59 eV),
27 indicating an increasing grazing pressure on phytoplankton under warming conditions.
28 Although the difference is consistent with that reported in previous studies, it is very
29 likely to arise from another reason, i.e., differential proximities of the optimal
30 temperature (T_{opt} in nonlinear temperature responses of rates) of phytoplankton and
31 microzooplankton to the environmental temperature, as we found that the environmental
32 temperature is closer to the optimal temperature of phytoplankton growth than to that of
33 microzooplankton grazing in this subtropical environment. Our results suggest that

34 nonlinear temperature responses of plankton should be considered when evaluating and
35 predicting the effects of ocean warming on ecosystem productivity and food web
36 dynamics, especially in subtropical and tropical waters.

37

38 **Introduction**

39 Marine phytoplankton plays a vital role in marine food web and global
40 biogeochemical cycling (Field et al. 1998). How marine primary production and the
41 efficiency of marine biological pump will respond to ocean warming strongly depends on
42 the effect of temperature on phytoplankton growth (Sarmiento et al. 2004; Taucher and
43 Oschlies 2011; Cael and Follows 2016). Temperature can affect phytoplankton through
44 both bottom-up and top-down controls. For example, enhanced upper-ocean stratification
45 in a warming ocean reduces nutrient supply, resulting in the decline of primary
46 production and phytoplankton biomass (Behrenfeld et al. 2006; Boyce et al. 2010).

47 Meanwhile, marine zooplankton grazing activities exert a top-down control on
48 phytoplankton, which is also temperature dependent (Rose and Caron 2007). According
49 to the Metabolic Theory of Ecology (MTE; Brown et al. 2004), the temperature
50 sensitivity, in terms of activation energy (E_a , eV), is lower for autotrophic processes (~
51 0.32 eV), such as phytoplankton growth, than for heterotrophic processes (~ 0.65 eV),
52 such as zooplankton grazing activity and respiration (Allen et al. 2005; López-Urrutia et

53 al. 2006; Chen et al. 2012). If this were true, warming may exacerbate the top-down
54 control on phytoplankton biomass, contributing to the decrease of primary production,
55 which ultimately affects the functioning and services of marine ecosystem. This point has
56 been used to explain the common occurrence of phytoplankton blooms in cold waters
57 (Rose and Caron 2007; López-Urrutia 2008) and to predict a more heterotrophic ocean
58 under projected ocean warming because more CO₂ will be released with increasing
59 upper-ocean temperature (Brown et al. 2004; López-Urrutia et al. 2006). However, the
60 difference of temperature sensitivity between autotrophic and heterotrophic rates is still
61 contentious, partly because the estimate of temperature sensitivity is sensitive to the
62 method used.

63 The widely used temperature sensitivity ($Q_{10} = 1.88$) is estimated from the Eppley
64 curve by fitting the upper envelope of the maximum growth rate of phytoplankton and
65 temperature in a laboratory dataset including all kinds of species (Eppley 1972; Rose and
66 Carron 2007; Bissinger et al. 2008). Instead of focusing on the envelope relationships
67 across all species, some studies suggested to consider the average rates of species under

68 different temperatures, and applied the ordinary least squares (OLS) regression to fit
69 average growth rate vs. temperature in the laboratory dataset (Sal and López-Urrutia
70 2011). These studies provided evidence for a lower temperature sensitivity of autotrophic
71 processes, which were used to predict warming effect on marine ecosystems. However,
72 the problems hidden in the statistical approach used in the above-mentioned studies when
73 analyzing the dataset should not be ignored (Chen and Laws 2017). The OLS regression
74 used in previous studies was usually applied on a pooled dataset including all data pairs
75 of rates and temperatures to estimate the activation energy without considering the errors
76 in the predictor (X) and the interdependence among the residuals. As a rule of thumb, the
77 rates measured for the same taxa or assemblages at different temperatures are more
78 correlated with each other than with those of different taxa or assemblages at different
79 temperatures. Thus, using a single regression on a pooled dataset, which contains the
80 rates of both the same and different taxa or assemblages, usually violates the assumption
81 of the OLS about the independence of the residuals, resulting in an underestimate of
82 temperature sensitivity (Chen and Laws 2017). For example, a single OLS regression on

83 a pooled dataset of fast-growing diatoms, which can dominate in cold environments, and
84 of slow-growing cyanobacteria, which tend to dominate in warm environments, will
85 underestimate the regression slope and hence the temperature sensitivity. Thus, a more
86 appropriate method to estimate the temperature sensitivity is to average the responses of
87 individual species to temperatures within a physiologically relevant range (Dell et al.
88 2011), with the results suggesting that there may be no difference in mean intraspecific
89 temperature sensitivity between phytoplankton and zooplankton (Chen and Liu 2015,
90 Chen and Laws 2017).

91 Although the median values of the intraspecific E_a between phytoplankton growth
92 rate and zooplankton grazing rate are similar, it does not mean that their E_a should be the
93 same for all communities. Some analysis based on laboratory culture data suggested that
94 there is great variability in the E_a of phytoplankton growth around the median value of
95 0.65 eV, and it varies among different phytoplankton taxa (Dell et al. 2011; Chen and
96 Laws 2017). Kremer et al. (2017) also found that the estimate of temperature sensitivity
97 was affected by phytoplankton functional groups. Thus, when estimating the temperature

98 sensitivity of in situ phytoplankton communities, a preferable approach is to measure E_a
99 of natural plankton assemblages instead of laboratory species, to take the community
100 composition into consideration. When quantifying the temperature sensitivity of natural
101 assemblages, it is also inappropriate to run a single regression for a pooled dataset
102 consisting of data pairs collected from different locations at different time points (Rose
103 and Caron 2007; Chen et al. 2012; Regaudie-De-Gioux and Duarte 2012), due to similar
104 statistical problems involved in the analysis of laboratory data (Chen and Laws 2017).
105 The key is that the assemblages used in the analysis should have similar compositions.
106 For now, the best approach might be to run short-term temperature modulation
107 experiments to circumvent the issue of community composition shift as shown in Vaquer-
108 Sunyer & Duarte (2013) and Chen & Liu (2015), although acclimation may be a problem
109 in such experiments. Our previous study at a subtropical coastal site using such approach
110 (Chen and Liu 2015) provided useful insights into thermal response of the natural
111 phytoplankton community dominated by diatoms. However, to generalize these patterns,
112 we need to investigate the temperature sensitivity of plankton in various environments.

113 One important component of the present study is to examine the responses of
114 different size classes of phytoplankton to temperature. Size is usually regarded as the
115 master trait of phytoplankton (Lichtman and Klausmeier 2008). There are ongoing
116 debates about the role of temperature in affecting phytoplankton size structure. Marañón
117 and his colleagues (Marañón et al. 2013, 2014, 2015) strongly believed that nutrient
118 supply rather than temperature plays the overriding role in determining phytoplankton
119 size structure, while some scientists argued that the effect of temperature cannot be
120 totally neglected (Lopez-Urrutia and Morán 2015; Ward 2015). Nonetheless, all the
121 above-mentioned studies relied on correlations of chlorophyll with temperature and
122 nutrients. The best evidence should come from the comparison between nutrient- and
123 temperature-related growth rates of different size classes. As previous studies have
124 already pointed out that pico-phytoplankton, especially cyanobacteria, has a higher
125 temperature sensitivity than larger phytoplankton (Kulk et al. 2012; Chen et al. 2014;
126 Chen and Laws 2017), we expect that different phytoplankton size classes will respond
127 differently to the same temperature variation.

128 With the above points in mind, we compared the acute responses of phytoplankton
129 growth rate and microzooplankton grazing rate to short-term temperature modulations at
130 two contrasting subtropical sites in the Hong Kong coastal waters. One site (Western
131 Estuarine Station, or WE) is located in the downstream of the Pearl River and is
132 dominated by large phytoplankton, such as diatoms, due to its eutrophic environment
133 (Chen et al. 2009). The other site (Eastern Oceanic Station, or EO) is jointly affected by
134 the China Coastal Current and oceanic water from the South China Sea, where the
135 phytoplankton community is usually nutrient-limited and is dominated by cyanobacteria
136 *Synechococcus* in summer. The dilution technique, the most commonly used method to
137 directly measure phytoplankton specific growth rate and microzooplankton grazing rate
138 simultaneously (Landry and Hassett 1982; Calbet and Landry 2004; Laws 2013), was
139 applied to measure phytoplankton growth rate and grazing loss rate of the whole
140 phytoplankton community and three different size classes (micro-, nano-, and pico-
141 phytoplankton) at five different temperatures in a range possibly including the
142 temperature optima of constituent species. We aim to find out the thermal responses of

143 growth rate and grazing loss rate of natural phytoplankton assemblages, and to test the
144 following hypothesis: cyanobacteria should have a higher temperature sensitivity than
145 other phytoplankton, which can affect the temperature sensitivity of the whole
146 phytoplankton community. Therefore, the temperature sensitivity of phytoplankton
147 community at Station EO, which is dominated by small phytoplankton, should be higher
148 than that at Station WE, which is dominated by large phytoplankton. We expect that at
149 the eutrophic station WE, the average temperature sensitivity should be roughly equal
150 between phytoplankton growth and microzooplankton grazing, while at Station EO
151 dominated by small phytoplankton, the temperature sensitivity of phytoplankton growth
152 should be a little higher than that of microzooplankton grazing, particularly for the small
153 size classes.

154 **Materials and Methods**

155 *Study sites and measurements of environmental parameters*

156 We evaluated the impacts of temperature on phytoplankton growth rate and
157 microzooplankton grazing rate at Station WE (22° 21.32'N, 113° 56.78'E) and Station EO

158 (22° 20.45'N, 114° 17.70'E), both in the Hong Kong coastal waters. These two stations
159 have distinct hydrographic and trophic characteristics (Fig. 1). Experiments were
160 conducted monthly from May 2016 to April 2017. Water temperature and salinity were
161 measured using a YSI EXO2 multi-probe sensor, which was calibrated before each
162 sampling. Surface sea water (*ca.* 30 L) was collected in the polycarbonate carboys from
163 these two stations, and brought back to the laboratory for the following experiments. The
164 samples for inorganic nutrients were collected from the sea water filtered through a 0.2
165 µm filter capsule, stored in -20°C freezer, and thawed at room temperature prior to
166 analysis. Inorganic nutrient concentrations including nitrate, nitrite, ammonia, phosphate,
167 and silicate were measured using a Skalar auto-analyzer (San Plus system, Netherlands)
168 in the laboratory according to the JGOFS protocol.

169 *Phytoplankton size structure measurements*

170 Phytoplankton were divided into three size classes by filtering 250 mL sea water
171 sequentially through 20, 2, and 0.2 µm polycarbonate membrane filters (GVS
172 Corporation) using a vacuum pump under low pressure. The phytoplankton retained on

173 the 20, 2, and 0.2 μm filters were defined as micro-, nano-, and pico-phytoplankton,
174 respectively (Sieburth et al. 1978; Marañón et al. 2001). The biomass of each size class
175 was represented by Chlorophyll *a* (Chl *a*) concentration, which was measured following
176 the JGOFS protocol. After filtration, each filter was immediately stored in a freezer at -
177 80°C until further treatment. For pigment extraction, the filters were soaked in 5 mL 90%
178 acetone at -20°C in the darkness for 20 hours. After the extraction, the samples were
179 centrifuged to remove detritus, and the suspensions were then used for measuring
180 fluorescence using a Turner Designs Model 7200 fluorometer with a non-acidification
181 module. The fluorometer was checked against a solid standard each time before
182 measurement (Strickland and Parsons 1972; Ducklow and Dickson 1994). The total
183 phytoplankton biomass was the sum of Chl *a* concentrations of the three size classes.

184 *Short-term temperature modulation experiments*

185 Phytoplankton growth rate and microzooplankton grazing rate were estimated at five
186 different temperatures using the dilution technique (Landry and Hassett 1982). The
187 temperatures for the experiments were set up according to *in situ* ambient temperature T,

188 which was measured using a YSI EXO2 multi-probe sensor when collecting sea water: T
189 $- 5^{\circ}\text{C}$, $T - 3^{\circ}\text{C}$, $T^{\circ}\text{C}$, $T + 3^{\circ}\text{C}$, and $T + 5^{\circ}\text{C}$. In summer, $T - 7^{\circ}\text{C}$ instead of $T + 5^{\circ}\text{C}$ was
190 used to minimize the problem of high temperature inhibition. In the dilution experiments,
191 through diluting the natural sea water with filtered sea water at the same site to several
192 proportions and incubating the bottles for 24 hours, the net growth rate of phytoplankton
193 can be calculated. Assuming that phytoplankton growth rate is unaffected by the dilution,
194 and microzooplankton grazing rate is proportional to the fraction of natural sea water,
195 both rates can be estimated through the linear regression of net growth rate against the
196 dilution factors (the proportion of the original unfiltered sea water). In this study, we used
197 two dilution treatments (15% and 100% of natural sea water) in duplicates of 1.2 L PC
198 bottles, known as “two-point” dilution technique, which was modified from the original
199 dilution approach and has been shown to be as accurate as the standard dilution approach
200 (Landry et al. 1984; Strom and Fredrickson 2008; Sherr et al. 2013; Chen 2015a).

201 In each set of dilution experiments (five sets for five temperatures in total), sea
202 water was filtered using a $0.2\ \mu\text{m}$ filter capsule (Pall Corporation) to obtain particle-free

203 sea water, and was added into two 1.2 L polycarbonate bottles to a prescribed volume.

204 These bottles were then filled with unfiltered sea water to full capacity to get a mixture of

205 85% particle-free sea water and 15% unfiltered sea water that contained natural plankton.

206 Duplicate 1.2 L polycarbonate bottles filled with unfiltered sea water were prepared for

207 the 100% dilution treatment (100% natural seawater). During this process, unfiltered sea

208 water in carboy was gently stirred occasionally and distributed to bottles as evenly as

209 possible. To ensure sufficient nutrients for phytoplankton growth, especially under higher

210 temperature incubation conditions, nutrients (NO_3^- : $10 \mu\text{mol L}^{-1}$, PO_4^{3-} : $1 \mu\text{mol L}^{-1}$ in

211 final concentration) were added into all experimental bottles. Extra duplicated bottles of

212 100% unfiltered seawater without nutrient amendment were also prepared and incubated

213 under *in situ* temperatures to evaluate the influence of adding nutrients. Then, all the

214 bottles were capped tightly and placed in an incubator that has five independent enclosed

215 shelves with different temperatures (FIRSTEK) for 24 hours. All five shelves shared the

216 same light intensity of approximately $100 \mu\text{mol photons m}^{-2} \text{ s}^{-1}$, which simulated the

217 average *in situ* light intensity experienced by phytoplankton in the nature, and a light:

218 dark cycle of 14:10. The samples for determining Chl *a* concentrations of three size
219 classes (size - fractionated Chl *a*) were collected from the initial unfiltered seawater, as
220 well as from each bottle after incubation as described above. Samples for determining
221 cell abundances of pico-phytoplankton including *Synechococcus* and pico-eukaryotes
222 were also collected before and after incubation, and analyzed using a Becton-Dickson
223 FACSCalibur flow cytometer (details are given in the Supplementary Information).
224 Experimental equipment including carboys, filters, bottles, and tubing was acid-washed
225 with 10% HCl, followed by Milli-Q and *in situ* sea water rinses before each experiment.

226 *Estimates of growth rate and grazing rate*

227 Growth rates and grazing mortality rates of the total phytoplankton and three size
228 classes were estimated following Landry et al. (2008). Briefly, by assuming exponential
229 growth for phytoplankton, the net growth rate (k) in each bottle was calculated as
230 $(1/t)\ln(P/dP_0)$, where P is the final biomass of the total phytoplankton and/or each of the
231 three size classes of phytoplankton, which is represented by Chl *a* concentration or cell
232 abundance of pico-phytoplankton, P_0 is the initial phytoplankton biomass/abundance, d is

233 the dilution factor (15% or 100%) of each bottle, and t is the duration of incubation time
234 (24 hours). The intrinsic growth rate (μ_n ; d^{-1}) and mortality grazing rate (m ; d^{-1}) of
235 phytoplankton were determined from the linear regression between net growth rate (k)
236 and dilution factor (d) by assuming an identical intrinsic phytoplankton growth rate in
237 each bottle. At *in situ* temperature, the instantaneous growth rate (μ_0 ; d^{-1}) was calculated
238 by adding the net growth rate of the bottles without adding nutrients to the mortality
239 grazing rate ($\mu_0 = m + k_{100\%}$ -without nutrient addition).

240 *Estimation of temperature sensitivity and optimal temperature (T_{opt})*

241 According to the MTE, the Boltzmann-Arrhenius (BA) model of biochemical reaction
242 kinetics can be used to predict thermal responses of metabolism-linked rates within a
243 physiological temperature range (PTR; the temperature range below optimal temperature)
244 (Gillooly et al. 2001; Pawar et al. 2016). For the metabolism-linked rate (R), i.e., the
245 phytoplankton growth rate or microzooplankton grazing rate, the model can be described
246 as follows:

$$247 \quad R = R_0 e^{\frac{-E_a}{k_b T}} \quad (1)$$

248 where R_0 is the normalization coefficient that includes the effect of body size, E_a is the
 249 activation energy (eV) that indicates temperature sensitivity, k_b is Boltzmann's constant
 250 (8.617×10^{-5} eV K⁻¹), and T is temperature in Kelvin (K). After logarithmically
 251 transforming the terms on both sides of Eq. (1), the activation energy (E_a) was estimated
 252 as the slope of linear regression of the log-transformed rate against the Boltzmann
 253 temperature $-1/k_b T$ (Brown et al. 2004; Kremer et al. 2017).

254 As the thermal responses of metabolism-linked rates are usually unimodal in a
 255 sufficiently wide temperature range, a unimodal extension of the BA model (Johnson and
 256 Lewin 1946; Dell et al. 2011; Chen and Laws 2017) is used to describe the relationship
 257 between metabolism-linked rates and temperature in a temperature range without
 258 restricting the data to the PTR:

$$259 \quad r = r_0 \frac{e^{\frac{E_a}{k_b}(\frac{1}{T_0} - \frac{1}{T})}}{1 + \frac{E_a}{E_h - E_a} e^{\frac{E_h}{k_b}(\frac{1}{T_{opt}} - \frac{1}{T})}} \quad (2)$$

260 where T_{opt} is the optimal temperature, at which the rate reaches the maximum value; E_h is
 261 added to describe the “steepness” of the decrease of the rate at higher temperature than T_{opt} ,
 262 and E_a determines how fast the rate increases with temperature below T_{opt} , which shares

263 the same definition with the linear model mentioned above. r is the growth rate or grazing
264 rate at temperature T . r_0 is the normalization constant. Other items are the same as those in
265 *Eq. (1)*.

266 In the majority of our experimental groups, the relationship between phytoplankton
267 growth rate (or microzooplankton grazing rate) and temperature within the 10-degree
268 thermal range was unimodal. *Eq. (2)* was used to fit the data in each set of experiments.
269 Nevertheless, sometimes the estimated values of E_a and E_h were extremely high with high
270 variance because the temperature range used in the model was relatively small and most of
271 the data located around the peak of the curve, which only allowed robust estimate of the
272 optimal temperature (T_{opt}). Insufficient sampling of temperature range was due to the
273 limitation of the short-term incubation experiments on natural communities. We had to
274 limit the experimental temperatures to a small range to avoid deteriorating the plankton
275 community and to be ecologically realistic. Practically, the number of temperature
276 treatments was restricted by resource and limited manpower. Therefore, the unimodal
277 function was only used in the estimate of T_{opt} but not of E_a .

278 The BA model was applied to estimate E_a of phytoplankton growth rate and
279 microzooplankton grazing rate through fitting the rate vs. temperature data within the PTR.
280 The data were restricted to the PTR by removing the rates that surpassed the optimal
281 temperature from every temperature modulated experiment. Totally, 13 sets of experiments
282 were conducted at each station, and 37% and 34% of the total data of phytoplankton
283 community growth rate and microzooplankton grazing rate were excluded from the
284 calculation. The E_a of each set of experiments was calculated through an OLS linear
285 regression. As the E_a values at each station varied randomly without apparent seasonal
286 pattern (Fig. S1), we used the linear mixed effects model treating months as random effects
287 associated with E_a to estimate the average E_a at each station. This model allows random
288 variations of both slope and intercept to account for hierarchical data structure, and has
289 been applied in some studies on data analysis related to MTE (Van de Pol and Wright 2009;
290 Bates et al. 2014; Kremer et al. 2017). The model for phytoplankton growth rate can be
291 described as follows:

$$292 \ln v_{i,j} = (\ln v_0 + \lambda D_i + \theta_{vi}) + \frac{E_{av} + \beta D_i + \theta_{Eavi}}{k_b} \left(\frac{1}{T_0} - \frac{1}{T_{i,j}} \right) + \varepsilon_{i,j} \quad (3)$$

293 where $v_{i,j}$ is the growth rate of total phytoplankton or each of the three size classes at the
 294 j^{th} temperature $T_{i,j}$ in the i^{th} experiment; v_0 is the normalization coefficient at reference
 295 temperature T_0 (288.15K); E_{av} is the mean activation energy for phytoplankton growth
 296 rate; and θ_{vi} and θ_{Eavi} represent the deviations of intercept ($\ln v_0$) and slope (E_{av}) in
 297 the i^{th} experiment from the mean, respectively. D_i is a dummy variable indicating the
 298 station information. D_i is set to 0 at Station EO, and to 1 at Station WE. Thus, λ and β are
 299 the differences in intercept and slope, respectively, between the two stations. Since we
 300 incubated all bottles at the same light condition and added the same concentration of
 301 nutrients (to ensure phytoplankton growth), we did not include the effects of light and
 302 nutrient in this model.

303 To calculate the temperature sensitivity of microzooplankton grazing rate,
 304 microzooplankton biomass was added to the model as follows:

$$305 \ln m_{i,j} = \alpha \ln(MZ_i) + (\ln m_0 + \lambda D_i + \theta_{mi}) + \frac{E_{am} + \beta D_i + \theta_{Eami}}{k_b} \left(\frac{1}{T_0} - \frac{1}{T_{i,j}} \right) + \varepsilon_{i,j} \quad (4)$$

306 where $m_{i,j}$ is the microzooplankton grazing rate at the j^{th} temperature $T_{i,j}$ in i^{th} experiment,
 307 m_0 is the normalization coefficient at reference temperature T_0 (288.15K); E_{am} is the mean

308 activation energy for microzooplankton grazing rate; θ_{mi} and θ_{Eami} represent the
309 random effects of intercept ($\ln m_0$) and slope (E_{am}) in the i^{th} experiment, respectively; MZ
310 is the microzooplankton biomass in carbon units ($\mu\text{g C L}^{-1}$) in the i^{th} experiment, which
311 was estimated based on the microscopic enumeration and bio-volume measurement of the
312 microzooplankton in each experiment (details are in Supplementary Information); and α is
313 a constant describing the relationship between grazing rate (m) and biomass (MZ). Dummy
314 variable (D_i) representing the station information is also included in this model as in Eq.
315 (3).

316 All statistical analyses were performed using the software R 3.1.2 (Team 2014). The
317 nonlinear regression analysis was applied using the R function “*nls*”. The linear mixed
318 effects model was performed using “*lmer*” in R package “*lme4*”. The conditional R^2 and
319 marginal R^2 were calculated to assess the goodness of the fit of the model using
320 “*r.squaredGLMM*” in the R package “*MuMIn*” (Nakagawa and Schielzeth 2013). To
321 compare the activation energies among size classes at each station, Welch’s ANOVA (R
322 function “*oneway.test*”) was used instead of the classic one-way ANOVA because the data

323 violated the assumption of homogeneity of variance. Finally, Welch's *t*-test was performed
324 to identify the difference of activation energies between every group and every other group
325 of rates. (Ruxton et al. 2006).

326 **Results**

327 *Environmental condition and phytoplankton size structure*

328 Pronounced seasonality was observed at both stations. Sea surface temperatures at
329 the two stations varied similarly (Fig. 2), but the concentrations of inorganic nutrients
330 differed dramatically between the two stations (Table S1). Both total dissolved inorganic
331 nitrogen (TIN, the total concentration of nitrate, nitrite, and ammonia) and phosphate
332 concentration at Station WE were remarkably higher (*ca.* 8-fold higher) than those at
333 Station EO. Total Chl *a* concentration was also much higher at Station WE (7.58 ± 8.53
334 $\mu\text{g L}^{-1}$, range: 0.97-30.31 $\mu\text{g L}^{-1}$) than at Station EO ($3.14 \pm 1.89 \mu\text{g L}^{-1}$, range: 1.13-7.06
335 $\mu\text{g L}^{-1}$) (Fig. 2). Micro-phytoplankton (> 20 μm) accounted for the major proportion of
336 the phytoplankton biomass at both stations, and were more dominant at Station WE (WE:
337 $44\% \pm 28\%$; EO: $38\% \pm 23\%$). Total Chl *a* concentration was positively correlated with

338 the concentration of micro-phytoplankton at Station WE, while it was correlated with the
339 concentration of nano-phytoplankton at Station EO, where nano-phytoplankton
340 accounted for $30\% \pm 16\%$ of the total. Flow cytometric analysis demonstrated that
341 *Synechococcus* was more abundant in summer at both stations, and their cell
342 concentrations were positively correlated with temperatures (Spearman rank correlation
343 test, for EO, $r = 0.91$, $p < 0.001$; for WE, $r = 0.95$, $p < 0.001$) (Fig. S2).

344 *Temperature sensitivity of phytoplankton community growth rate and grazing mortality*
345 *rate by microzooplankton*

346 Monthly E_a varied randomly without any discernable trend at both stations (Fig. S1).
347 Based on the linear mixed effects model (Eqs. 3, 4), the mean E_a of the whole
348 phytoplankton growth rate was 0.35 eV (95% CI = 0.24 to 0.46 eV) at Station EO and
349 was 0.37 eV (95% CI = 0.27 to 0.48 eV) at Station WE (Table 1, Fig. 3). No significant
350 difference was found between these two stations (p value for β in Eq. 3: $p > 0.05$), which
351 contrasted with our initial expectation. Both fixed and random effects in the mixed effects
352 model explained about 90% variance of the whole phytoplankton community growth rate,

353 but only ~50% of the total variance can be interpreted by the fixed effects at each station,
354 which suggested the importance of random effects (Table 1).

355 Surprisingly, microzooplankton biomass did not play a significant role in the model
356 predicting grazing rate at Station EO ($\chi^2 = 0.45, p > 0.05$). Although it was found
357 significant at Station WE ($\chi^2 = 6.23, p < 0.05$), the results were not much different from
358 the ones without microzooplankton biomass (Welch's *t*-test, $p > 0.05$). Hence, the
359 variable of microzooplankton biomass was removed from the models. The average E_a of
360 microzooplankton grazing rate also showed no significant difference between the two
361 stations (EO: 0.64 eV, 95% CI = 0.38 to 0.89 eV; WE: 0.57 eV, 95% CI = 0.36 to 0.78
362 eV; p value for β in *Eq. 4*: $p > 0.05$; Table 2, Fig. 4), which agreed with the canonic value
363 (0.65 eV) of MTE at both stations.

364 At each station, E_a of bulk phytoplankton growth rate was significantly lower than
365 that of microzooplankton grazing rate (Welch's *t*-test, EO: $p = 0.037 < 0.05$; WE: $p =$
366 $0.019 < 0.05$; Fig. 5), which again differed from our hypothesis. As such, the percentage
367 of phytoplankton consumed by microzooplankton, which is represented by $m: \mu$ (Calbet

368 and Landry 2004), increased with rising temperature in each group. The result of the
369 linear mixed effects model using Eq. (3) on $m: \mu$, exhibiting the distance in activation
370 energy between growth rate and grazing rate ($\Delta E_a = E_m - E_\mu$), was 0.30 eV (95% CI =
371 0.16 to 0.44 eV), which further supported that microzooplankton grazing rate was more
372 sensitive to temperature increase compared with phytoplankton growth rate.

373 *Temperature sensitivity of growth rate and grazing mortality rate by microzooplankton of*
374 *three size classes of phytoplankton*

375 The mean E_a values of phytoplankton growth rate at both stations differed for the
376 three size classes (Table 1, Fig. 5). At Station WE, only micro-phytoplankton growth rate
377 was less sensitive to temperature increase than the grazing rate (0.34 eV, 95% CI = 0.25
378 to 0.43 eV, Table 1, Fig. S3a). This was consistent with the whole phytoplankton
379 community growth rate (Welch's t -test, $p > 0.05$) due to the dominance of micro-
380 phytoplankton. The E_a values of nano- and pico-phytoplankton growth rates were slightly
381 higher than that of the whole phytoplankton community (Table 1; Welch's t -test, nano: p
382 = 0.009 < 0.01; pico: $p = 0.047 < 0.05$). While at Station EO, E_a of pico-phytoplankton

383 growth rate was the closest to that of the whole phytoplankton community (0.31 eV, 95%
384 CI = 0.16 to 0.46 eV; Welch's t -test, $p > 0.05$), and the growth rate of micro-
385 phytoplankton had a significantly higher value than that of the whole phytoplankton (0.52
386 eV, 95% CI = 0.33 to 0.7 eV, Welch's t -test, $p = 0.001 < 0.01$). However, E_a of micro-
387 phytoplankton may be biased because of its data structure (Fig S3a). In the estimate of E_a ,
388 since data should be restricted to below optimal temperature to meet the requirement of
389 the BA model, there were only two data points remained in some groups. Estimates based
390 on restricted dataset in which at least three points were required were also carried out to
391 examine the accuracy of our results (Table S2). No significant changes were observed in
392 these estimates except for E_a of micro-phytoplankton growth rate with a value of 0.22 eV
393 (95% CI = 0.06 to 0.38 eV). Therefore, more observations were required to confirm the
394 E_a value of micro-phytoplankton growth rate at Station EO. The temperature sensitivity
395 of *Synechococcus* was significantly greater than that of the whole phytoplankton
396 community and that of pico-phytoplankton at both stations (Welch's t -test, $p < 0.001$;
397 Fig. 5). These results were in concordance with previous studies (Kulk et al. 2012; Chen

398 et al. 2014; Stawiarski et al. 2016; Chen and Laws 2017), which revealed that
399 cyanobacteria has a lower growth rate but higher temperature sensitivity than large
400 eukaryotic phytoplankton such as diatoms.

401 No pronounced difference was found in E_a of microzooplankton grazing rates of
402 three size classes at Station EO (Welch's ANOVA, $p > 0.05$). The E_a value of grazing
403 rate on nano-phytoplankton was slightly higher than that of nano-phytoplankton growth
404 rate (Welch's t -test, $p = 0.038 < 0.05$; Fig. 5). At Station WE, the grazing rate on nano-
405 phytoplankton had a high E_a value (0.97 eV, 95% CI = 0.57 to 1.37 eV, Fig. S4b). The E_a
406 values for the other size classes and *Synechococcus* showed no obvious differences from
407 that for the grazing rates on community and were close to the predicted values.

408 *Optimal temperatures of phytoplankton growth rate and grazing mortality rate by*
409 *microzooplankton*

410 The nonlinear least-squares regression model was used to fit the data of each set of
411 experiments when there was a unimodal relationship between growth rate (or grazing
412 rate) and temperature (solid lines in Figs. 3, 4). The optimal temperatures for growth rate

413 and grazing rate were obtained from the nonlinear models. The overall mean optimal
414 temperature of phytoplankton community growth rate was $23.7 \pm 3.2^\circ\text{C}$, significantly
415 lower than that of microzooplankton grazing rate ($25.9 \pm 4^\circ\text{C}$; paired t-test, $df = 20$, $p =$
416 $0.013 < 0.05$; Fig. 6). The optimal temperatures of both growth rate and grazing rate were
417 positively correlated with the environmental temperature (growth rate: $r = 0.88$, $df = 23$, p
418 < 0.001 ; grazing rate: $r = 0.88$, $df = 20$, $p < 0.001$; Fig. S5). For the three phytoplankton
419 size classes, their growth rates showed slightly lower optimal temperatures compared
420 with corresponding grazing rates, but the difference was not significant. For
421 *Synechococcus* and pico-eukaryotes, no difference was observed in the optimal
422 temperatures between growth rate and grazing rate.

423 **Discussion**

424 *Implications of different thermal sensitivity of phytoplankton growth rate and*
425 *microzooplankton grazing rate*

426 Predicting how marine primary production, the efficiency of biological pump and
427 food web stability respond to the projected warming entails reliably quantifying the

428 temperature sensitivity of various plankton rates, especially phytoplankton growth rate.

429 Accurately estimating the temperature sensitivity requires us to be aware of the potential

430 statistical problems in previous analyses (Chen and Laws 2017). In the current study, we

431 used a short-term temperature modulation approach to minimize the statistical problems

432 as much as possible, and to circumvent the issue of community structure shift under

433 warming conditions. Our results showed that at the community level, the average

434 temperature sensitivity of phytoplankton growth rate was 0.35 eV, lower than that of

435 microzooplankton grazing rate at the two contrasting stations in the subtropical coastal

436 waters. At the face value, this difference seems consistent with the classic conception of

437 lower temperature sensitivity of autotrophs (Allen et al. 2005; Rose and Caron 2007;

438 Yvon-Durocher et al. 2010; Chen et al. 2012; Regaudie-De-Gioux and Duarte 2012),

439 which has strong implications for the effect of warming on some critical ecosystem

440 processes, such as net community production (López-Urrutia et al. 2006; Regaudie-De-

441 Gioux and Duarte 2012) and the efficiency of the biological pump (Laws et al. 2000;

442 Cael and Follows 2016). Different thermal responses of phytoplankton and their

443 predators would also affect the dynamics and stability of marine food webs under global
444 warming (Vasseur and McCann 2005; Rose and Caron 2007; Fussmann et al. 2014). Due
445 to the lower temperature sensitivity, more phytoplankton biomass would subject to
446 microzooplankton grazing as temperature increases, which would reduce possible
447 occurrences of phytoplankton blooms under warming in the eutrophic coastal waters
448 (Rose and Caron 2007; Cloern 2018). Nevertheless, the above speculations are based on
449 projected transient responses. In the future, it is necessary to take into account thermal
450 adaptive behaviors of phytoplankton for predicting warming effects on plankton
451 ecosystems (García et al. 2018).

452 *Why is phytoplankton temperature sensitivity lower? – Influence of optimal temperature*
453 *on estimating activation energy*

454 It is intriguing that our results still predict lower E_a of phytoplankton than that of
455 microzooplankton even though we tried our best to minimize the statistical problems and
456 took into account the influences of community composition (Chen and Laws 2017). We
457 believe that the main reason is related to the effects of optimal temperature (T_{opt}) of

458 growth rate. Based on the nonlinear thermal response function that is extended from the

459 Arrhenius equation (Johnson and Lewin 1946; Dell et al. 2011; Chen and Laws 2017):

460
$$\ln\mu = \ln\mu_0 + \frac{E_a}{k_b} \left(\frac{1}{T_0} - \frac{1}{T} \right) - \ln \left[1 + \frac{E_a}{E_h - E_a} e^{\frac{E_h}{k_b} \left(\frac{1}{T_{opt}} - \frac{1}{T} \right)} \right] \quad (5)$$

461 it is clear that the apparent slope of the linear regression of log-transformed growth rate

462 $(\ln\mu)$ against Boltzmann temperature $\left(\frac{1}{k_b} \left(\frac{1}{T_0} - \frac{1}{T} \right) \right)$ is affected not only by E_a but also by

463 T_{opt} . When $T \ll T_{opt}$, the apparent linear slope is close to E_a . But when T approaches T_{opt} ,

464 the last term in Eq. (5) becomes significantly positive, leading to reduction of the

465 apparent linear slope. When $T > T_{opt}$, the slope eventually becomes negative. In addition,

466 the apparent linear slope also depends on the temperature range of the experiments,

467 which is necessarily small in our studies due to the concern of short-term thermal shock.

468 This phenomenon has been observed previously (Pawar et al. 2016). It has been

469 repeatedly reported that T_{opt} of many organisms including phytoplankton becomes closer

470 to environmental temperature in warm environments (Deutsch et al. 2008; Huey et al.

471 2009; Thomas et al. 2012; Chen 2015b). As a consequence, the reduced sensitivity of

472 phytoplankton growth rate to temperature should be a universal pattern in subtropical and
473 tropical environments.

474 The observed differences of temperature sensitivity (i.e., the apparent E_a estimated
475 from the linear regression), hence, can be well explained by the discrepancy of T_{opt}
476 between microzooplankton and phytoplankton. T_{opt} of microzooplankton grazing rate
477 (17.3-32.2°C) was higher than that of phytoplankton growth rate (18.2-29.6°C) in our
478 study (Fig. 6). Thus, higher T_{opt} of microzooplankton relative to the environment
479 temperature T in Eq. (5) would result in a higher apparent linear slope compared with that
480 of phytoplankton. Physiologically, the lower T_{opt} of phytoplankton might be related to the
481 substantial requirement for RubiscoCO enzyme at high temperature (Flynn and Raven
482 2016). In laboratory experiments, it is also true that T_{opt} of zooplankton was higher than
483 that of phytoplankton or even cannot be observed in some designed experimental
484 temperature range (Renaud et al. 2002; Chen and Laws 2017). Difference in the optimal
485 temperatures between phytoplankton and microzooplankton holds the potential to
486 influence the dynamics of microbial food web under climate warming. The

487 microzooplankton grazing rate would keep rising to reach its maximum when
488 temperature increases, while the phytoplankton growth is prone to deviate away from its
489 best fitness because it is more likely that the increased temperature can surpass the
490 optima. Thus, more phytoplankton biomass would be consumed by enhanced
491 microzooplankton grazing activities in a warming future. In addition, the ratio of $m:\mu$,
492 which represents the grazing impact of microzooplankton on phytoplankton, also
493 increases with temperature and has a high optimal temperature ($26.2 \pm 3.6^\circ\text{C}$), indicating
494 an increasing grazing pressure on phytoplankton under warming conditions. Interestingly,
495 Boersma et al. (2016) suggested that when going up the trophic level, fish also seem to
496 have much higher T_{opt} than phytoplankton under the same environmental temperature.
497 Further considering the evolution of endothermy, we suspect that as organisms evolve
498 from unicellular to more complicated forms that confer them maintain a higher body
499 temperature than the environment, their T_{opt} might also evolve to be higher to take
500 advantage of the greater fitness under higher temperature (Huey and Kingsolver 1989).

501 It is a challenging question why in our earlier investigation (Chen and Liu 2015), few
502 incidences of T_{opt} were observed for both phytoplankton and microzooplankton (i.e., the
503 rates kept increasing with temperature in most experiments). The most likely reason is
504 that T_{opt} was much higher than the environmental temperature in the study region
505 investigated in Chen & Liu (2015), leaving few opportunities to capture T_{opt} within the
506 designed experimental temperature range. Some studies have suggested a considerably
507 larger discrepancy between the environmental temperature and optimal temperature for
508 the phytoplankton living in polar and temperate waters where the annual mean
509 temperature is under $\sim 25^{\circ}\text{C}$ (see Fig. 2A in Thomas et al. 2012). Although the study
510 region in Chen & Liu (2015) was in the subtropical waters, the annual mean temperature
511 ($20.2 \pm 5.4^{\circ}\text{C}$) was lower than 25°C , and also lower compared with that of the current
512 study region ($25 \pm 4.3^{\circ}\text{C}$). In addition, the study site in Chen & Liu (2015) was extremely
513 eutrophic, with nitrate concentration always exceeding $15 \mu\text{mol L}^{-1}$. It was also found
514 that less nutrient availability can reduce T_{opt} for phytoplankton (Thomas et al. 2017).

515 Thus, the lower T_{opt} observed in the present study probably is related to the mesotrophic
516 nature of the study region.

517 *Different temperature sensitivities among three size classes of phytoplankton at the two*
518 *stations*

519 Community composition plays an important role in determining the temperature
520 sensitivity of phytoplankton growth rate in natural environments (Chen and Laws 2017).

521 We hypothesized that the phytoplankton community at Station EO dominated by small
522 phytoplankton, mainly by cyanobacteria, would be more sensitive to temperature increase
523 than that at Station WE, which was dominated by larger phytoplankton such as diatoms.

524 However, the estimated E_a for phytoplankton growth rate of the whole community was
525 not significantly different at the two stations, and was lower than that of

526 microzooplankton grazing rate (Tables 1, 2, Fig. 5). This suggests that the influence of

527 nonlinear temperature response (i.e., T_{opt}) is much greater than that of community

528 structure.

529 The E_a value of phytoplankton growth rate varied among different size classes or
530 groups. Nano- and pico-phytoplankton growth rates showed higher E_a than micro-
531 phytoplankton growth rate at Station WE (Fig. 5b), which could drive an increase in the
532 contribution of small phytoplankton to the bulk biomass, and shift the community
533 structure under climate warming. It has also been shown that small phytoplankton
534 increased with increasing temperature in mesocosm experiments using either marine and
535 freshwater plankton communities (Sommer and Lengfellner 2008; Yvon-Durocher et al.
536 2011). The underlying mechanism could be a combination of faster response of small
537 phytoplankton to warmer temperature and enhanced grazing pressure on large
538 phytoplankton due to the difference in temperature sensitivities between micro-
539 phytoplankton and their predators (Fig. 5). Because small phytoplankton are less prone to
540 sinking and would accelerate nutrient regeneration by stimulating the growth of
541 microzooplankton, ocean warming, by shifting the phytoplankton community to smaller
542 sizes, would reduce the efficiency of carbon export (Laws et al. 2000).
543 *Cyanobacteria having high temperature sensitivity*

544 The estimated activation energy of *Synechococcus* growth rate was consistently high
545 at both stations (EO: 0.58 eV, 95% CI = 0.36 to 0.80 eV; WE: 0.54 eV, 95% CI = 0.41 to
546 0.67 eV; Fig. 5), close to the canonic value of 0.65 eV and in line with previous studies of
547 both freshwater and marine cyanobacteria (Joehnk et al. 2008; Chen et al. 2014; Chen
548 and Laws 2017). It has also been found that several eukaryotic strains isolated from the
549 oligotrophic ocean have lower temperature coefficient (Q_{10}) than pico-prokaryotes,
550 including *Synechococcus* and *Prochlorococcus* (Kulk et al. 2012; Stawiarski et al. 2016).
551 Similar results were observed at Station EO (Fig. 5a), which is closer to the open ocean.
552 Some studies pointed out that cyanobacteria have relatively higher T_{opt} than pico-
553 eukaryotes, which relieves them from high temperature inhibition in (sub)tropical
554 environments (Chen et al. 2014; Chen and Laws 2017). Thus, it is not surprising to find
555 its peak abundance in summer in coastal waters (Fig. S2; Agawin et al. 1998; Chen et al.
556 2009; Chen et al. 2014), and its abundance increases with rising annual mean temperature
557 under nutrient-sufficient conditions (Li 1998).

558 *Potential problems in the estimate of E_a in such short-term temperature modulation*

559 *experiments*

560 Every methodology may have its own bias or drawback. For the incubation method
561 we used, one problem might be the latent influence of the resource supply such as light
562 and nutrients on the estimate of E_a . The effects of temperature on phytoplankton growth
563 usually interact with light and nutrients. The interactive effects on growth are
564 complicated as they are not simple combination of additive effects (Thomas et al. 2017).
565 Practically, this study focused on the effect of temperature on phytoplankton growth
566 under replete resource supply. Thus, additional nutrients were added to ensure sufficient
567 nutrients for phytoplankton growth. Although the light intensity (about 100 $\mu\text{mol photons}$
568 $\text{m}^{-2} \text{s}^{-1}$) used in the experiments may not be sufficient for some phytoplankton species
569 during the incubation, especially when temperature increases (Collins and Boylen 1982),
570 it was assumed to be saturating irradiance for the growth of phytoplankton community in
571 some studies (Edwards et al. 2016). We also assumed that the effect of light should be
572 negligible in the estimate of E_a in our study. Actually, as the light intensity was set to

573 imitate the *in situ* situation experienced by the phytoplankton, which were continuously
574 mixed within the mixed layer at a time scale less than 24 hours (Franks 2015; Chen and
575 Smith 2018), our estimates could be more relevant to the *in situ* conditions. Recent
576 studies found that nutrient-limitation or light-limitation would reduce the optimal
577 temperature of phytoplankton growth and diminish the temperature sensitivity (Edwards
578 et al. 2016; Thomas et al 2017). If so, the lower temperature sensitivity and optimal
579 temperature for phytoplankton growth found in the current study may be more critical
580 when involving the effects of resource supply in the real ocean.

581 Another problem is the possible damage to plankton community caused by the
582 temperature manipulation especially temperature extremes, which could impose “thermal
583 shock” to the plankton. To alleviate this problem, the experimental temperature gradients
584 were prudently designed to be confined to small deviations from the *in situ* temperature.
585 The experimentally elevated temperatures would not cause damage to the majority of
586 plankton in our experiments because significant increase of phytoplankton biomass can
587 be observed after incubation. Our estimates of E_a were consistent with many previous

588 studies, such as Laws et al. (2000), Allen et al. (2005), Lopez-Urrutia et al. (2006), Rose
589 and Caron (2007), Cael and Follows (2016), and Kremer et al. (2017), although for
590 different reasons, which suggested that the problem of temperature manipulation did not
591 bias the estimate of E_a substantially. However, the restricted temperature range might
592 lead to high variation (uncertainty) of the estimates of E_a . Moreover, as ocean warming is
593 very slow relative to warming used in the experimental design, the results of such short-
594 term experiments should be applied cautiously in predicting the effects of warming on the
595 marine plankton on a long-term scale. Despite the above-mentioned issues of short-term
596 experiments, our estimates provide some useful information about the temperature
597 sensitivity, which is an important trait of the plankton community to predict how the
598 marine ecosystem responds to ocean warming.

599 **Conclusion**

600 Our results suggest that the heterotrophs are more sensitive to the increase of
601 temperature than the autotrophs in the subtropical regions even when the statistical
602 problems were minimized and the community composition was taken into consideration

603 in our experiments. This difference arises due to a new problem that is the different
604 discrepancies of the optimal temperature of phytoplankton and microzooplankton to the
605 environmental temperature. It does not suggest the above-mentioned statistical problems
606 do not occur in previous studies.

607 Our study highlights the importance of considering nonlinear temperature responses
608 when estimating the temperature sensitivity of plankton in the subtropical and tropical
609 regions, where environmental temperatures are often close to the optimal temperature of
610 phytoplankton, but probably less so for zooplankton. This has significant implications for
611 the impact of global warming on ocean ecosystems. We expect that warming will
612 continue to shift phytoplankton to small size (cyanobacteria) and microzooplankton will
613 probably flourish, leading to a more active microbial loop. How these repercussions will
614 affect key ocean ecosystem functioning, such as the marine biological pump or fishery,
615 remains important tasks for oceanographers and ecologists.

616

617 **References**

- 618 Agawin, N. S. R., C. M. Duarte, and S. Agusti. 1998. Growth and abundance of
619 *Synechococcus* sp. in a Mediterranean Bay: seasonality and relationship with
620 temperature. *Mar. Ecol. Prog. Ser.* **170**: 45-53. doi: 10.3354/meps170045
- 621 Allen, A. P., J. F. Gillooly, and J. H. Brown. 2005. Linking the global carbon cycle to
622 individual metabolism. *Funct. Ecol.* **19**: 202-213. doi: 10.1111/j.1365-
623 2435.2005.00952.x
- 624 Bates, D., M. Maechler, B. Bolker, and S. Walker. 2014. lme4: Linear mixed-effects
625 models using Eigen and S4. R package version **1**: 1-23.
- 626 Behrenfeld, M. J., R. T. O'Malley, D. A. Siegel, C. R. McClain, J. L. Sarmiento, G. C.
627 Feldman, A. J. Milligan, P. G. Falkowski, R. M. Letelier, and E. S. Boss. 2006.
628 Climate-driven trends in contemporary ocean productivity. *Nature* **444**: 752-755.
629 doi: 10.1038/nature05317
- 630 Bissinger, J. E., D. J. Montagnes, J. harples, and D. Atkinson. 2008. Predicting marine
631 phytoplankton maximum growth rates from temperature: Improving on the Eppley

632 curve using quantile regression. *Limnol. Oceanogr.* **53**(2), 487-493. doi:
633 10.4319/lo.2008.53.2.0487

634 Boersma, M., N. Grüner, N. T. Signorelli, P. E. M. González, M. A. Peck, and K. H.
635 Wiltshire 2016. Projecting effects of climate change on marine systems: is the mean
636 all that matters? *Proc. R. Soc. B*, **283**(1823), 20152274. doi:
637 10.1098/rspb.2015.2274

638 Boyce, D. G., M. R. Lewis, and B. Worm. 2010. Global phytoplankton decline over the
639 past century. *Nature* **466**: 591-596. doi: 10.1038/nature09268

640 Brown, J. H., J. F. Gillooly, A. P. Allen, V. M. Savage, and G. B. West. 2004. Toward a
641 metabolic theory of ecology. *Ecology* **85**: 1771-1789. doi: 10.1890/03-9000

642 Cael, B. B. and M. J. Follows. 2016. On the temperature dependence of oceanic export
643 efficiency. *Geophys. Res. Lett.* **43**(10): 5170-5175. doi: 10.1002/2016GL068877

644 Calbet, A., and M. R. Landry. 2004. Phytoplankton growth, microzooplankton grazing,
645 and carbon cycling in marine systems. *Limnol. Oceanogr.* **49**: 51-57. doi:
646 10.4319/lo.2004.49.1.0051

647 Chen, B. Z., M. R. Landry, B. Q. Huang, and H. B. Liu. 2012. Does warming enhance the
648 effect of microzooplankton grazing on marine phytoplankton in the ocean? *Limnol.*
649 *Oceanogr.* **57**: 519-526. doi: 10.4319/lo.2012.57.2.0519

650 Chen, B. Z., and E. A. Laws. 2017. Is there a difference of temperature sensitivity between
651 marine phytoplankton and heterotrophs? *Limnol. Oceanogr.* **62**: 806-817. doi:
652 10.1002/lno.10462

653 Chen, B. Z., H. B. Liu, B. Q. Huang, and J. Wang. 2014. Temperature effects on the growth
654 rate of marine picoplankton. *Mar. Ecol. Prog. Ser.* **505**: 37-47. doi:
655 10.3354/meps10773

656 Chen, B. Z., H. B. Liu, M. R. Landry, M. Chen, J. Sun, L. Shek, X. H. Chen, and P. J.
657 Harrison. 2009. Estuarine nutrient loading affects phytoplankton growth and
658 microzooplankton grazing at two contrasting sites in Hong Kong coastal waters.
659 *Mar. Ecol. Prog. Ser.* **379**: 77-90. doi: 10.3354/meps07888

- 660 Chen, B. Z., and K. L. Liu. 2015. Responses of autotrophic and heterotrophic rates of
661 plankton from a subtropical coastal site to short-term temperature modulations. *Mar.*
662 *Ecol. Prog. Ser.* **527**: 59-71. doi: 10.3354/meps11218
- 663 Chen, B. Z. 2015a. Assessing the accuracy of the “two-point” dilution technique. *Limnol.*
664 *Oceanogr.: Methods.* **13**: 521-526. doi: 10.1002/lom3.10044
- 665 Chen, B. Z. 2015b. Patterns of thermal limits of phytoplankton. *J. Plankton Res.* **37**(2),
666 285-292. doi:10.1093/plankt/fbv009
- 667 Chen, B. Z., S. L. Smith, and K. W. Wirtz. 2018. Effect of phytoplankton size diversity on
668 primary productivity in the North Pacific: trait distributions under environmental
669 variability. *Ecol. Lett.* doi:10.1111/ele.13167
- 670 Cloern, J. E. 2018. Why large cells dominate estuarine phytoplankton. *Limnol. Oceanogr.*
671 **63**(S1): S392-S409. doi: 10.1002/lno.10749
- 672 Collins, C. D., and C. W. Boylen. 1982. Physiological responses of *Anabaena variabilis*
673 (Cyanophyceae) to Instantaneous Exposure to Various combinations of light

674 intensity and temperature. *J. Phycol* 18(2), 206-211. doi:10.1111/j.1529-
675 8817.1982.tb03175.x

676 Dell, A. I., S. Pawar, and V. M. Savage. 2011. Systematic variation in the temperature
677 dependence of physiological and ecological traits. *Proc. Natl. Acad. Sci. USA* **108**:
678 10591-10596. doi: 10.1073/pnas.1015178108

679 Deutsch, C. A., J. J. Tewksbury, R. B. Huey, K. S. Sheldon, C. K. Ghalambor, D. C. Haak,
680 and P. R. Martin. 2008. Impacts of climate warming on terrestrial ectotherms across
681 latitude. *Proc. Natl. Acad. Sci. USA* **105**: 6668-6672. doi:
682 10.1073/pnas.0709472105

683 Ducklow, H., and A. Dickson. 1994. Chapter 14. Measurement of chlorophyll a and
684 paeopigments by fluorometric analysis, p. 119-122. In A. Knap, A. Michaels, A.
685 Close, H. Ducklow, and A. Dickson. [eds.], *Protocols for the Joint Global Ocean*
686 *Flux Study (JGOFS) core measurements*. UNESCO.

687 Edwards, K. F., M. K. Thomas, C. A. Klausmeier, and E. Litchman. 2016. Phytoplankton
688 growth and the interaction of light and temperature: A synthesis at the species and
689 community level. ? *Limnol. Oceanogr.* **61**(4), 1232-1244. doi: 10.1002/lno.10282

690 Eppley, R. W. 1972. Temperature and phytoplankton growth in the sea. *Fish. bull.* **70**(4),
691 1063-1085.

692 Field, C. B., M. J. Behrenfeld, J. T. Randerson, and P. Falkowski. 1998. Primary production
693 of the biosphere: Integrating terrestrial and oceanic components. *Science* **281**: 237-
694 240. doi: 10.1126/science.281.5374.237

695 Franks, P. J. 2014. Has Sverdrup's critical depth hypothesis been tested? Mixed layers vs.
696 turbulent layers. *ICES J Mar. Sci.* **72**(6), 1897-1907. doi: 10.1093/icesjms/fsu175

697 Flynn, K. J., and J. A. Raven, 2016. What is the limit for photoautotrophic plankton growth
698 rates? *J. Plankton Res.* **39**(1), 13-22. 10.1093/plankt/fbw067

699 Fussmann, K. E., F. Schwarzmüller, U. Brose, A. Jousset, and B. C. Rall. 2014. Ecological
700 stability in response to warming. *Nat. Clim. Change*, **4**(3), 206. doi:
701 10.1038/nclimate2134

702 García, F. C., E. Bestion, R. Warfield, and G. Yvon-Durocher. 2018. Changes in
703 temperature alter the relationship between biodiversity and ecosystem functioning.
704 Proc. Natl. Acad. Sci. USA. **115**(43), 10989-10994. doi: 0.1073/pnas.1805518115

705 Gillooly, J. F., J. H. Brown, G. B. West, V. M. Savage, and E. L. Charnov. 2001. Effects
706 of size and temperature on metabolic rate. Science **293**: 2248-2251. doi:
707 10.1126/science.1061967

708 Huey, R. B., and J. G. Kingsolver. 1989. Evolution of thermal sensitivity of ectotherm
709 performance. Trends Ecol. Evol. **4**(5), 131-135. doi: 10.1016/0169-
710 5347(89)90211-5

711 Huey, R. B., C. A. Deutsch, J. J. Tewksbury, L. J. Vitt, P. E. Hertz, H. J. Á. Pérez, and T.
712 Garland. 2009. Why tropical forest lizards are vulnerable to climate warming. Proc.
713 R. Soc. B **276**, 1939-1948. doi:10.1098/rspb.2008.1957

714 Joehnk, K. D., J. Huisman, J. Sharples, B. Sommeijer, P. M. Visser, and J. M. Stroom.
715 2008. Summer heatwaves promote blooms of harmful cyanobacteria. Glob. Chang.
716 Biol. **14**: 495-512. doi: 10.1111/j.1365-2486.2007.01510.x

- 717 Johnson, F. H., and I. Lewin. 1946. The growth rate of *E. coli* in relation to temperature,
718 quinine and coenzyme. *J. Cell. Physiol.* **28**: 47-75. doi: 10.1002/jcp.1030280104
- 719 Kremer, C. T., M. K. Thomas, and E. Litchman. 2017. Temperature-and size-scaling of
720 phytoplankton population growth rates: Reconciling the Eppley curve and the
721 metabolic theory of ecology. *Limnol. Oceanogr.* **62**(4), 1658-1670. doi:
722 10.1002/lno.10523
- 723 Kulk, G., P. de Vries, W. H. van de Poll, R. J. W. Visser, and A. G. J. Buma. 2012.
724 Temperature-dependent growth and photophysiology of prokaryotic and eukaryotic
725 oceanic picophytoplankton. *Mar. Ecol. Prog. Ser.* **466**: 43-55. doi:
726 10.3354/meps09898
- 727 Landry, M. R., and R. P. Hassett. 1982. Estimating the grazing impact of marine micro-
728 zooplankton. *Mar. Biol.* **67**: 283–288. doi:10.1007/BF00397668
- 729 Landry, M. R., S. L. Brown, Y. M. Rii, K. E. Selph, R. R. Bidigare, E. J. Yang, and M. P.
730 Simmons. 2008. Depth-stratified phytoplankton dynamics in Cyclone Opal, a

731 subtropical mesoscale eddy. *Deep-Sea Res. II* **55**: 1348-1359. doi:
732 10.1016/j.dsr2.2008.02.001

733 Landry, M. R., L. W. Haas, and V. L. Fagerness. 1984. Dynamics of Microbial Plankton
734 Communities - Experiments in Kaneohe Bay, Hawaii. *Mar. Ecol. Prog. Ser.* **16**:
735 127-133. doi: 10.3354/meps016127

736 Laws, E. A., P. G. Falkowski, J. W. O. Smith, H. Ducklow, and J. J. McCarthy. 2000.
737 Temperature affects export production in the open ocean. *Global Biogeochem.*
738 *Cycles.* **14**: 1231–1246. doi:10.1029/1999GB001229

739 Laws, E. A. (2013). Evaluation of in situ phytoplankton growth rates: a synthesis of data
740 from varied approaches. *Annu. Rev. Mar. Sci.* **5**, 247-268. doi: 10.1146/annurev-
741 marine-121211-172258

742 Li, W. K. 1998. Annual average abundance of heterotrophic bacteria and *Synechococcus*
743 in surface ocean waters. *Limnol. Oceanogr.* **43**(7), 1746-1753. doi:
744 10.4319/lo.1998.43.7.1746

- 745 Litchman, E., and C. A. Klausmeier. 2008. Trait-based community ecology of
746 phytoplankton. *Ann. Rev. Ecol. Evol. Syst.* **39**: 615-639. doi:
747 10.1146/annurev.ecolsys.39.110707.173549
- 748 López-Urrutia, Á., E. San Martín, R. P. Harris, and X. Irigoien. 2006. Scaling the metabolic
749 balance of the oceans. *Proc. Natl. Acad. Sci. USA* **103**: 8739-8744. doi:
750 10.1073/pnas.0601137103
- 751 López-Urrutia, Á. 2008. The metabolic theory of ecology and algal bloom formation.
752 *Limnol. Oceanogr.* **53**: 2046-2047. doi: 10.4319/lo.2008.53.5.2046
- 753 López-Urrutia, Á., and X. A. G. Morán. 2015. Temperature affects the size-structure of
754 phytoplankton communities in the ocean. *Limnol. Oceanogr.* **60**: 733–738. doi:
755 10.1002/lno.10049
- 756 Marañón, E., P. Cermeño, D. C. López-Sandoval, T. Rodríguez-Ramos, C. Sobrino, M.
757 Huete-Ortega, J. M. Blanco, and J. Rodríguez. 2013. Unimodal size scaling of
758 phytoplankton growth and the size dependence of nutrient uptake and use. *Ecol.*
759 *Lett.* **16**: 371-379. doi: 10.1111/ele.12052

760 Marañón, E., P. Cermeño, M. Huete-Ortega, D. C. López-Sandoval, B. Mouriño-
761 Carballido, and T. Rodríguez-Ramos. 2014. Resource supply overrides temperature
762 as a controlling factor of marine phytoplankton growth. *PLoS One* **9**: e99312. doi:
763 10.1371/journal.pone.0099312

764 Marañón, E., P. Cermeño, M. Latasa, and R. D. Tadonlécé. 2015. Resource supply alone
765 explains the variability of marine phytoplankton size structure. *Limnol. Oceanogr.*
766 **60**: 1848–1854. doi:10.1002/lno.10138

767 Marañón, E., P. M. Holligan, R. Barciela, N. González, B. Mouriño, M. J. Pazó, and M.
768 Varela. 2001. Patterns of phytoplankton size structure and productivity in
769 contrasting open-ocean environments. *Mar. Ecol. Prog. Ser.* **216**: 43-56. doi:
770 10.3354/meps216043

771 Morán, X. A. G., A. López-Urrutia, Á. Calvo-Díaz, and W. K. W. Li. 2010. Increasing
772 importance of small phytoplankton in a warmer ocean. *Glob. Chang. Biol.* **16**:
773 1137-1144. doi: 10.1111/j.1365-2486.2009.01960.x

- 774 Nakagawa, S., and H. Schielzeth. 2013. A general and simple method for obtaining R^2
775 from generalized linear mixed-effects models. *Methods Ecol. Evol.* **4**(2), 133-142.
776 doi: 10.1111/j.2041-210x.2012.00261.x
- 777 Pawar, S., A. I. Dell, V. M. Savage, and J. L. Knies. 2016. Real versus Artificial Variation
778 in the Thermal Sensitivity of Biological Traits. *Am. Nat.* **187**: E41-E52. doi:
779 10.1086/684590
- 780 Regaudie-De-Gioux, A., and C. M. Duarte. 2012. Temperature dependence of planktonic
781 metabolism in the ocean. *Global Biogeochem. Cycles* **26**: GB1015. doi:
782 10.1029/2010gb003907
- 783 Renaud, S. M., L. V. Thinh, G. Lambrinidis, and D. L. Parry. 2002. Effect of temperature
784 on growth, chemical composition and fatty acid composition of tropical Australian
785 microalgae grown in batch cultures. *Aquaculture*, **211**(1-4), 195-214. doi:
786 10.1016/S0044-8486(01)00875-4

787 Rose, J. M., and D. A. Caron. 2007. Does low temperature constrain the growth rates of
788 heterotrophic protists? Evidence and implications for algal blooms in cold waters.
789 *Limnol. Oceanogr.* **52**: 886-895. doi: 10.4319/lo.2007.52.2.0886

790 Ruxton, G. D. 2006. The unequal variance t-test is an underused alternative to Student's t-
791 test and the Mann–Whitney U test. *Beha. Ecol.* **17**(4), 688-690. doi:
792 10.1093/beheco/ark016

793 Sarmiento, J. L., R. Slater, R. Barber, L. Bopp, S. C. Doney, A. C. Hirst, J. Kleypas, R.
794 Matear, U. Mikolajewicz, P. Monfray, V. Soldatov, S. A. Spall, and R. Stouffer.
795 2004. Response of ocean ecosystems to climate warming. *Global Biogeochem.*
796 *Cycles* **18**: GB3003. doi: 10.1029/2003GB002134

797 Sherr, E. B., B. F. Sherr, and C. Ross. 2013. Microzooplankton grazing impact in the
798 Bering Sea during spring sea ice conditions. *Deep-Sea Res.* **II 94**: 57-67. doi:
799 10.1016/j.dsr2.2013.03.019

800 Sieburth, J. M., V. Smetacek, and J. Lenz. 1978. Pelagic ecosystem structure: heterotrophic
801 compartments of the plankton and their relationship to plankton size fractions.
802 *Limnol. Oceanogr.* **23**: 1256-1263. doi: 10.4319/lo.1978.23.6.1256

803 Sommer, U., and K. Lengfellner. 2008. Climate change and the timing, magnitude, and
804 composition of the phytoplankton spring bloom. *Global Change Biol.* **14**(6), 1199-
805 1208. doi: 10.1111/j.1365-2486.2008.01571.x

806 Stawiarski, B., E. T. Buitenhuis, and C. Le Quéré. 2016. The Physiological Response of
807 Picophytoplankton to Temperature and Its Model Representation. *Front. Mar. Sci.*
808 **3**: 164. doi: 10.1002/fno.10745

809 Strickland, J. D., and T. R. Parsons. 1972. A practical handbook of seawater analysis.

810 Strom, S. L., and K. A. Fredrickson. 2008. Intense stratification leads to phytoplankton
811 nutrient limitation and reduced microzooplankton grazing in the southeastern
812 Bering Sea. *Deep Sea Res.* **II 55**: 1761-1774. doi: 10.1016/j.dsr2.2008.04.008

813 Taucher, J., and A. Oschlies. 2011. Can we predict the direction of marine primary
814 production change under global warming? *Geophys. Res. Lett.* **38**: L02603. doi:
815 10.1029/2010gl045934

816 Team, R. C. 2014. *R: A Language and Environment for Statistical Computing*. Vienna: R
817 Foundation for Statistical Computing. Available online at: [http. www. R-project.](http://www.R-project.org)
818 [org.](http://www.R-project.org)

819 Thomas, M. K., C. T. Kremer, C. A. Klausmeier, and E. Litchman. 2012. A Global Pattern
820 of Thermal Adaptation in Marine Phytoplankton. *Science* **338**:1085-1088. doi:
821 10.1126/science.1224836

822 Thomas, M. K., C. T. Kremer, and E. Litchman. 2016. Environment and evolutionary
823 history determine the global biogeography of phytoplankton temperature traits.
824 *Glob. Ecol. Biogeogr.* **25**: 75-86. doi: 10.1111/geb.12387

825 Thomas, M. K., M. Aranguren-Gassis, C. T. Kremer, M. R. Gould, K. Anderson, C. A.
826 Klausmeier, and E. Litchman. 2017. Temperature–nutrient interactions exacerbate

827 sensitivity to warming in phytoplankton. *Global Change Biol.* **23**(8), 3269-3280.
828 doi:10.1111/gcb.13641

829 Van de Pol, M., and J. Wright. 2009. A simple method for distinguishing within-versus
830 between-subject effects using mixed models. *Anim. Behav.* **77**: 753-758. doi:
831 10.1016/j.anbehav.2008.11.006

832 Vaquer-Sunyer, R., and C. M. Duarte. 2013. Experimental Evaluation of the Response of
833 Coastal Mediterranean Planktonic and Benthic Metabolism to Warming. *Estuaries
834 Coasts* **36**: 697-707. doi: 10.1007/s12237-013-9595-2

835 Vasseur, D. A., and K. S. McCann. 2005. A mechanistic approach for modeling
836 temperature-dependent consumer-resource dynamics. *Am. Nat.* **166**(2), 184-198.
837 doi: 10.1086/431285

838 Ward, B. A. 2015. Temperature-correlated changes in phytoplankton community structure
839 are restricted to polar waters. *PloS one* **10**(8), e0135581. doi :
840 10.1371/journal.pone.0135581

841 Yang, Z., L. Zhang, X. Zhu, J. Wang, and D. J. Montagnes. 2016. An evidence-based
842 framework for predicting the impact of differing autotroph-heterotroph thermal
843 sensitivities on consumer-prey dynamics. *The ISME journal*, **10**(7), 1767. doi:
844 10.1038/ismej.2015.225

845 Yvon-Durocher, G., J. I. Jones, M. Trimmer, G. Woodward, and J. M. Montoya. 2010.
846 Warming alters the metabolic balance of ecosystems. *Phil. Trans. R. Soc. B* **365**:
847 2117-2126. doi: 10.1098/rstb.2010.0038

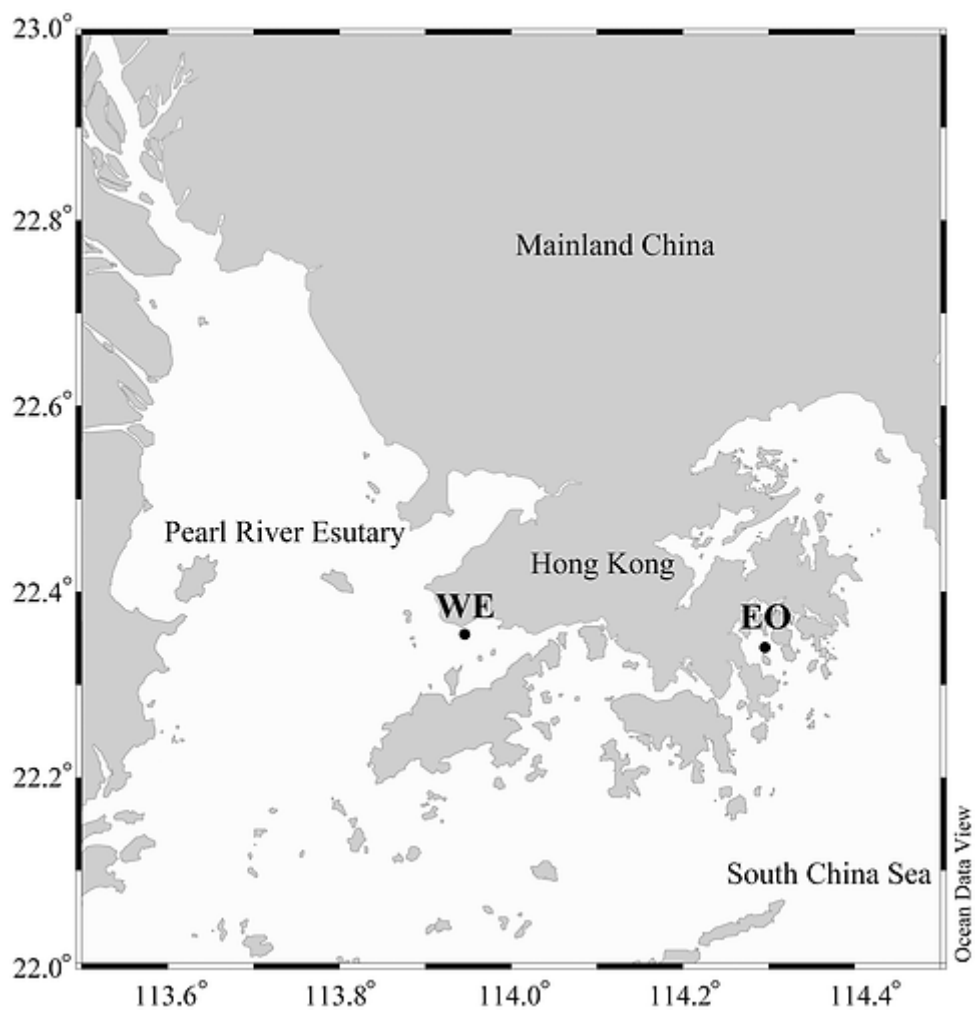
848 Yvon-Durocher, G., J. M. Montoya, V. Trimmer, and G. Woodward. 2011. Warming alters
849 the size spectrum and shifts the distribution of biomass in freshwater ecosystems.
850 *Global Change Biol.* **17**: 1681-1694, doi:10.1111/j.1365-2486.2010.02321.x
851

852 **Acknowledgments**

853 We sincerely thank three anonymous reviewers and M. R. Landry for helpful comments,
854 W. K. Lau and Y. F. YEUNG for their help with data sampling, and Z. J. Yu for editing
855 the manuscript. This study is supported by the National Basic Research Program
856 (“973” Program) of China (2015CB954003), Research Grants Council of the Hong Kong
857 Special Administrative Region, China (Project No. T21/602/16), Hong Kong Research
858 Grants Council (GRF-16128416 and 16101917 and RGC-NSFC joint scheme
859 N_HKUST609/15), and the State Key Lab on Marine Pollution (SKLMP) via the Seed
860 Collaborative Research Fund (SKLMP/SCRF/XXXX).

861

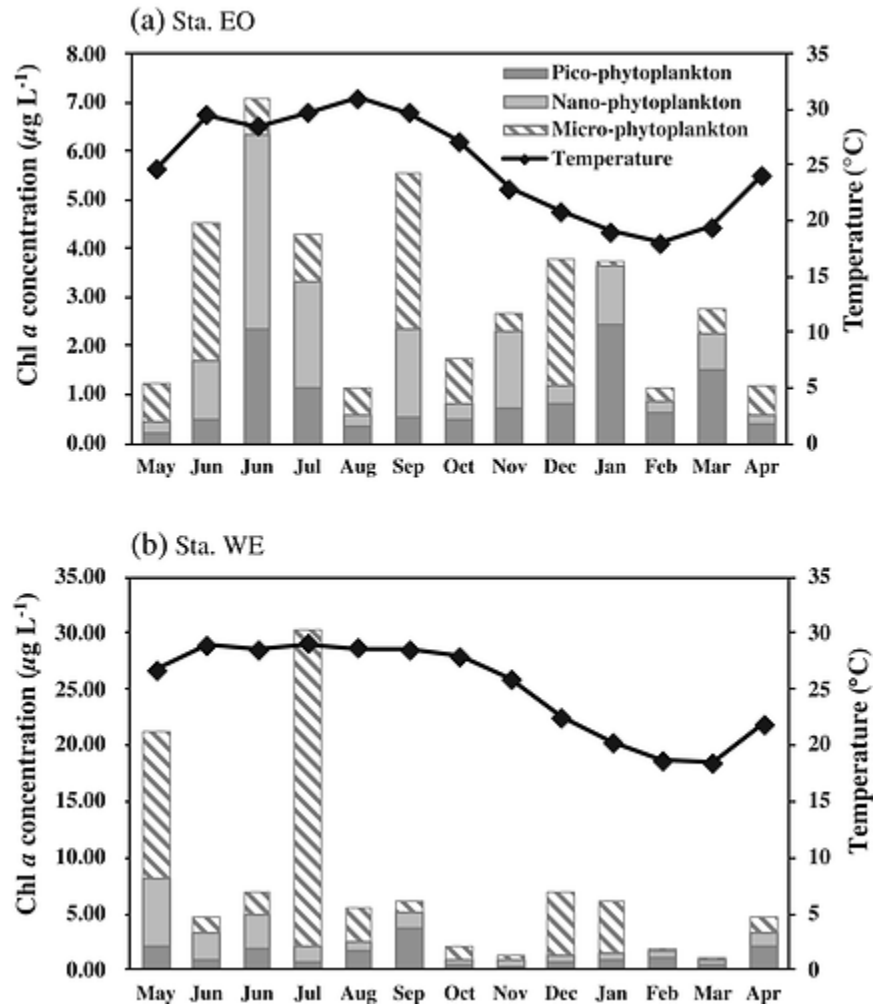
862 **Figures**



863

864 Fig. 1 Locations of study stations in Hong Kong waters. WE: Western Estuarine Station

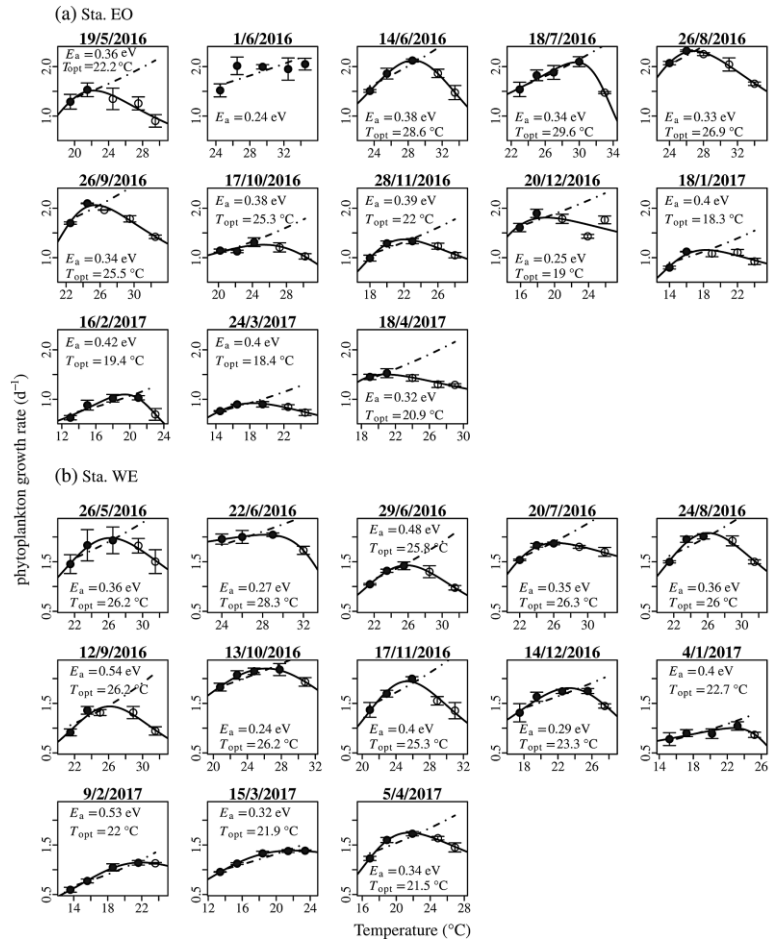
865 (22°21.32'N, 113°56.78'E); EO: Eastern Oceanic Station (22°20.45'N, 114°17.70'E).



866

867 Fig. 2 Monthly variations of temperature and chlorophyll *a* (Chl *a*) concentration of three

868 phytoplankton size classes at Station EO (a) and Station WE (b).



869

870

Fig. 3 Linear mixed effects model and nonlinear regression fits of phytoplankton

871

community growth rates and experimental temperature for individual experiments at

872

Station EO (a) and Station WE (b). The dash-dotted line is the fitted line of the

873

linear mixed effects model results, and the solid line is the fitted line of the nonlinear

874

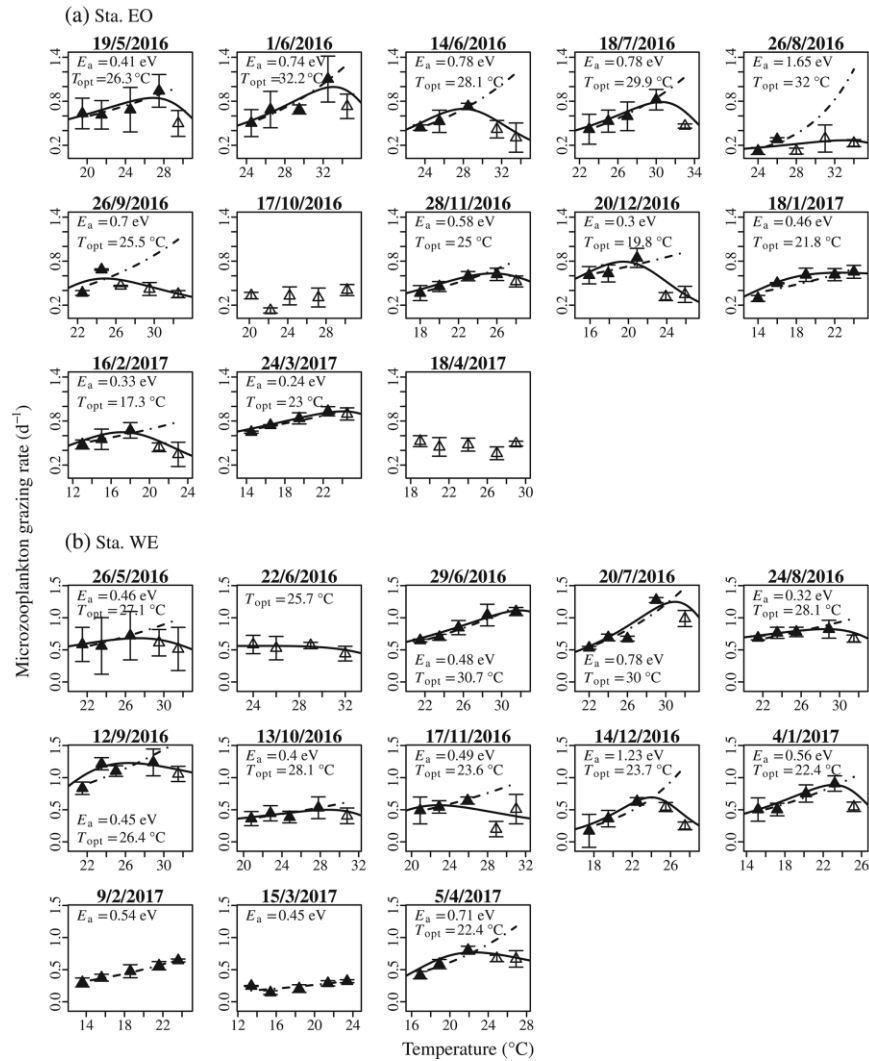
regression. Open circles: Data not used in the linear mixed effects model. E_a :

875

Activation energy obtained from the linear mixed effects model; T_{opt} : Optimal

876

temperature of growth rate obtained from the nonlinear regression.

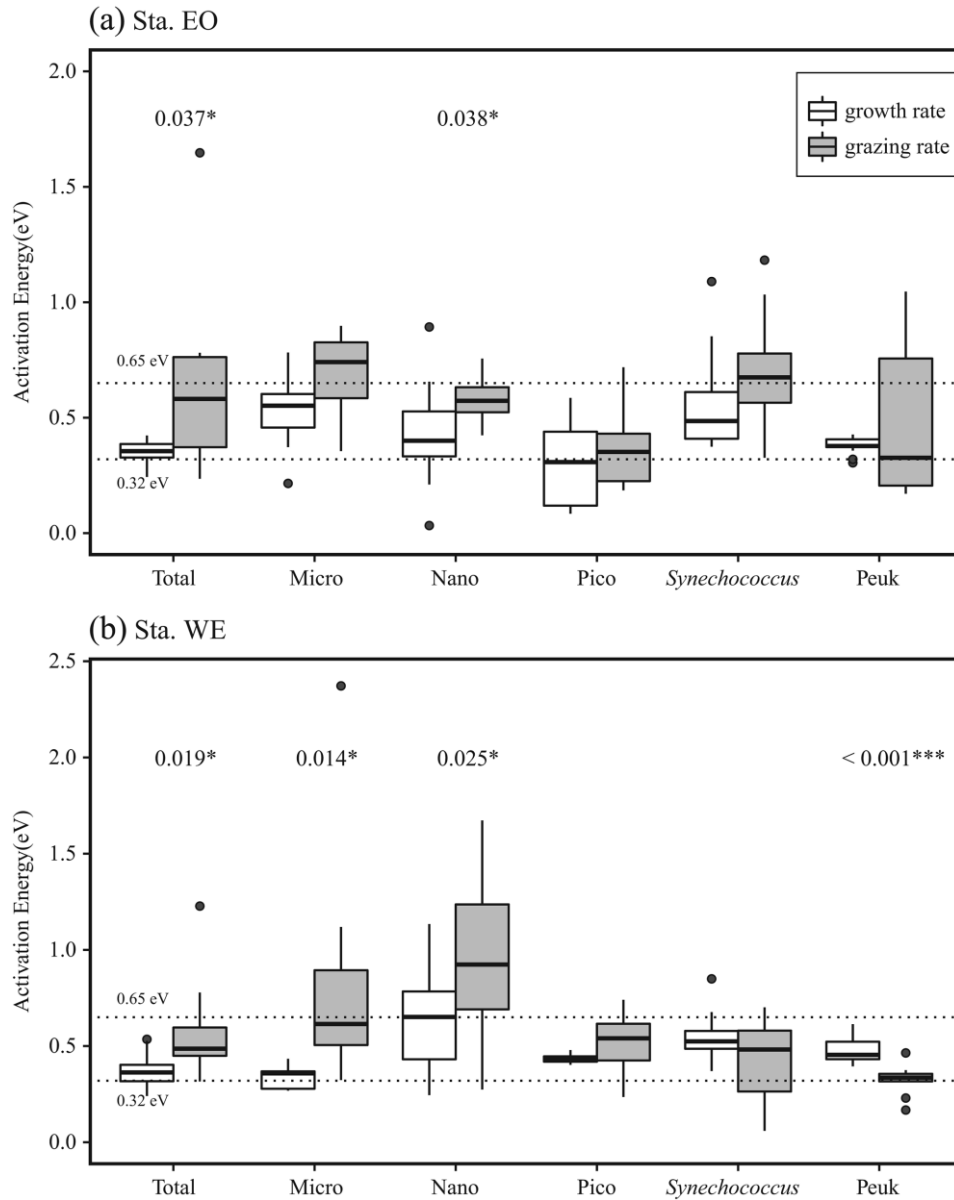


877

878 Fig. 4 Linear mixed effects model and nonlinear regression fits of microzooplankton

879 grazing rates on the total phytoplankton at experimental temperatures at station EO

880 (a) and station WE (b). Same as Fig. 3.



881

882 Fig. 5 Activation energies of growth rates of total phytoplankton, three size classes of

883 phytoplankton and two pico-phytoplankton and corresponding grazing mortality

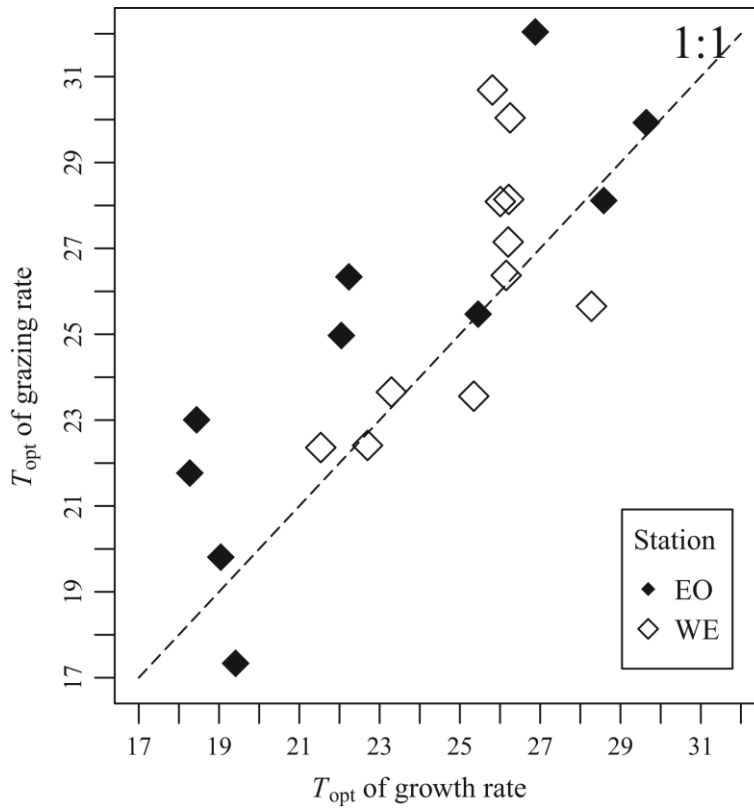
884 rates by microzooplankton at Station EO (a) and Station WE (b). The two dashed

885 lines represent the theoretical activation energies of autotrophic processes (0.32 eV)

886 and heterotrophic processes (0.65eV). Significant levels between activation energies

887 of growth rate and grazing rate are given by the p -values with the asterisks (* : $p <$

888 0.5; ** : $p < 0.1$; *** : $p < 0.001$).



889

890 Fig.6 Optimal temperatures of phytoplankton community growth rate and grazing

891 mortality rate by microzooplankton grazing. Dashed line is the 1:1 line.

892

893 Table 1. Estimated activation energies (E_a , eV) of total, three size classes, and taxa-specific phytoplankton growth rates derived from
894 the linear mixed effects model and OLS regression. The parameters of the linear mixed effects model include the average energy
895 (E_{av} , with 95% CI in brackets), the normalization constant ($\ln v_0 \pm$ standard error), standard deviations of the random effects of
896 $\ln v_0$ and E_{av} (θ_v and θ_{Eav}), percentage of variance explained by the random and fixed effect (V_{fr}), percentage of variance explained
897 by the fixed effect only (V_f), number of observations used in the model (N_o), and number of groups used in the model
898 (N_g). E_a (OLS) (eV) is the mean activation energy derived from the OLS regression, 95% CIs are in brackets.

Station	Growth rate	Linea mixed effects model								Linear model (OLS)
		$\ln \nu_0$	E_{av}	θ_ν	θ_{Eav}	V_{fr}	V_f	N_o	N_g	$E_{a(OLS)}$
EO station	Bulk phytoplankton	0.05 ± 0.11	0.35 (0.24, 0.46)	0.23	0.09	0.93	0.56	37	13	0.48 (0.32, 0.63)
	Micro-phytoplankton	-0.03 ± 0.11	0.52 (0.33, 0.70)	0.35	0.22	0.98	0.50	31	13	0.54 (0.39, 0.69)
	Nano-phytoplankton	-0.00 ± 0.15	0.43 (0.29, 0.57)	0.54	0.22	0.96	0.35	39	13	0.45 (0.34, 0.55)
	Pico-phytoplankton	-0.02 ± 0.12	0.31 (0.16, 0.46)	0.38	0.2	0.81	0.37	39	13	0.40 (0.23, 0.57)
	<i>Synechococcus</i> (FCM)	-0.83 ± 0.27	0.58 (0.36, 0.80)	0.9	0.23	0.97	0.19	40	13	0.88 (0.57, 1.19)
	Picoeukaryotes (FCM)	-0.15 ± 0.10	0.38 (0.29, 0.47)	0.31	0.04	0.95	0.29	42	13	0.44 (0.36, 0.52)
WE station	Bulk phytoplankton	0.02 ± 0.09	0.37 (0.27, 0.48)	0.29	0.12	0.92	0.41	44	13	0.47 (0.27, 0.66)
	Micro-phytoplankton	0.19 ± 0.08	0.34 (0.25, 0.43)	0.2	0.09	0.91	0.39	45	13	0.38 (0.29, 0.46)
	Nano-phytoplankton	-0.36 ± 0.11	0.63 (0.41, 0.84)	0.34	0.33	0.95	0.44	46	13	0.64 (0.43, 0.85)
	Pico-phytoplankton	-0.15 ± 0.14	0.43 (0.25, 0.61)	0.38	0.02	0.80	0.21	43	13	0.65 (0.34, 0.97)
	<i>Synechococcus</i> (FCM)	-0.15 ± 0.10	0.54 (0.41, 0.67)	0.3	0.14	0.88	0.65	42	13	0.69 (0.47, 0.9)
	Picoeukaryotes (FCM)	-0.06 ± 0.13	0.48 (0.35, 0.60)	0.38	0.07	0.94	0.36	35	12	0.65 (0.43, 0.87)

899

900

901 Table 2. Estimated activation energies (E_a , eV) of total, three size classes, and taxa-specific phytoplankton grazing mortality rates by
902 microzooplankton derived from the linear mixed effects model and OLS regression. The parameters of linear mixed effects
903 model include the average energy (E_{am} , with 95% CI in brackets), the normalization constants ($\ln m_0 \pm$ standard error), standard
904 deviations of the random effects of $\ln m_0$ and E_{am} (θ_m and θ_{Eam}), percentage of variance explained by the random and fixed effect
905 (V_{fr}); percentage of variance explained by the fixed effect only (V_f). Other parameters are the same with Table [1](#).

Station	Grazing rate	Linear mixed effects model								Linear model (OLS)
		$\ln m_0$	E_{am}	θ_m	θ_{Eam}	V_{fr}	V_f	N_o	N_g	$E_{a(OLS)}$
EO station	Bulk phytoplankton	-1.36 ± 0.31	0.64 (0.38, 0.89)	0.99	0.4	0.97	0.27	38	11	0.70 (0.39, 1.00)
	Micro-phytoplankton	-1.79 ± 0.52	0.45 (-0.34, 1.24)	1.03	0.75	0.58	0.09	25	8	1.78 (0.71, 2.85)
	Nano-phytoplankton	-1.31 ± 0.23	0.58 (0.34, 0.81)	0.57	0.09	0.78	0.29	39	10	0.86 (0.45, 1.27)
	Pico-phytoplankton	-0.70 ± 0.22	0.37 (0.16, 0.59)	0.62	0.19	0.78	0.22	39	11	0.59 (0.35, 0.82)
	<i>Synechococcus</i> (FCM)	-1.17 ± 0.27	0.69 (0.36, 1.03)	0.78	0.38	0.92	0.28	37	12	0.74 (0.45, 1.03)
	Picoeukaryotes (FCM)	-1.00 ± 0.30	0.49 (0.19, 0.80)	0.85	0.35	0.82	0.19	40	11	0.66 (0.18, 1.14)
WE station	Bulk phytoplankton	-1.11 ± 0.14	0.57 (0.36, 0.78)	0.44	0.3	0.91	0.40	47	12	0.61 (0.35, 0.87)
	Micro-phytoplankton	-1.83 ± 0.31	0.77 (0.40, 1.14)	1.07	0.6	0.94	0.28	50	13	0.66 (0.41, 0.91)
	Nano-phytoplankton	-1.44 ± 0.26	0.97 (0.57, 1.37)	0.76	0.54	0.87	0.44	45	12	1.12 (0.64, 1.60)
	Pico-phytoplankton	-0.43 ± 0.21	0.53 (0.32, 0.72)	0.62	0.17	0.90	0.22	39	12	0.72 (0.41, 1.03)
	<i>Synechococcus</i> (FCM)	-0.3 ± 0.16	0.43 (0.24, 0.63)	0.52	0.27	0.97	0.21	33	12	0.44 (0.27, 0.61)
	Picoeukaryotes (FCM)	-0.15 ± 0.18	0.33 (0.20, 0.46)	0.57	0.13	0.98	0.10	33	11	0.35 (0.23, 0.48)